Analysis of shear forces during mash disk formation

Problem presented by

Tom Bullock

PepsiCo Global Snacks R&D

ESGI145
CAMBRIDGE

ESGI145 was jointly hosted by

University of Cambridge

Isaac Newton Institute for Mathematical Sciences

Newton Gateway to Mathematics

Smith Institute for Industrial Mathematics and System Engineering

UNIVERSITY OF CAMBRIDGE
Centre for Mathematical Sciences

Isaac Newton Institute
for Mathematical Sciences

Newton Gateway
to Mathematics

Smith institute

with additional support from

Engineering and Physical Sciences Research Council

Innovate UK Knowledge Transfer Network

Cambridge University Press

University of Cambridge Faculty of Mathematics

University of Cambridge Centre for Mathematical Sciences

Report authors

Cameron Hall (University of Bristol), John Hinch (University of Cambridge),
Richard Purvis (University of East Anglia), Andrew Lacey (Heriot Watt University),
Yuri Sobral (Universidade de Brasilia), Gavin Moreton (University of East Anglia),
Michael Ewetola (Open University), John Ockendon (University of Oxford),
David Allwright (Smith Institute), Abishek Chakraborty (University of Cardiff),
Joaquim Correia (Universidade de Évora), Jose Cuminato (Universidade de São Paolo),
Karen Luong (University of Cambridge), Rita Teixeira da Costa (University of Cambrdige),
Yang Zhou (University of Bath)

Executive Summary

This report concerns a forming process in which mash is forced from a spreading manifold into moulds on a rotating drum, transported in the moulds underneath a surface held flush with the drum (the shoe), and ejected from the moulds. The quality of the final product is understood to be related to the shear stresses experienced by the mash in the moulds as it is transported under the shoe. We describe and analyse mathematical models of the forming process, focusing on the fluid mechanics of mash in a mould. We treat this as a driven cavity flow and obtain flow profiles, stress profiles, and expressions for the maximum shear stress for different rheological models of the mash (Newtonian fluid, power-law fluid, and Bingham plastic).

Contents

1 Introduction

PepsiCo Global Snacks manufactures a wide range of different products using an array of different techniques. In most cases, the manufacture of a given product will involve multiple steps, each of which may need to be optimised according to different metrics. One of the ways to achieve this optimisation is to use mathematical modelling. The development and analysis of mathematical models can be used to obtain quantitative insights into how different process parameters affect outputs such as the quality of the final product and the efficiency of the overall manufacturing system.

The problem presented at ESGI 145 concerns one specific process that is a step within more complicated manufacturing systems. In the process of concern, mash is taken from a continuous flow and moulded into disks. It is thought that the quality of the final product depends on the shear stresses experienced by the mash disk during this stage of processing. As a result, it is important to understand how different aspects of the moulding process affect the shear stresses experienced by the mash during the moulding process.

At the study group, we developed mathematical models to describe various aspects of the moulding process and we analysed these models to gain a better understanding of how the moulding process can best be controlled and modified. One important phenomenon explored during the study group was the flow of mash that occurs as the mash disks pass under a fixed surface called the "shoe", as depicted in Figure 1. During this step of the process, the mash disks are constrained within moulds on the surface of a rotating drum; as the mash-filled moulds move underneath the shoe, a flow of mash is induced by the difference in velocity between the moving moulds and the stationary shoe.
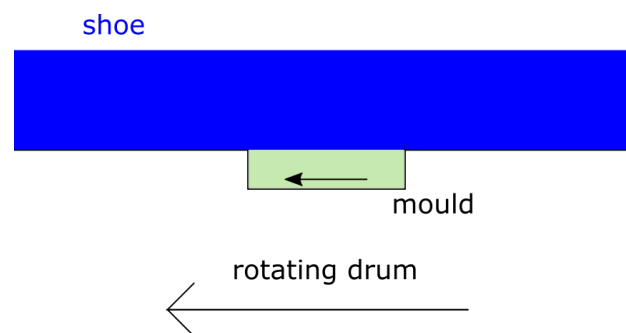

Figure 1: Schematic of a mash disk being transported under the shoe. As the process continues, the mash-filled mould is moved to the left by a rotating drum while the shoe remains stationary.

This report describes part of the work achieved at the study group, focusing on the mathematical analysis of the "flow under the shoe" outlined above. The report is divided into several sections. In Section 2, we describe the mathematical approach that we take

to modelling the flow under the shoe. In particular, we explain why a one-dimensional lubrication approximation of lid-driven cavity flow is an appropriate model to use, and we describe the mathematical structure of this problem.

In the following sections, we present mathematical solutions for the flow under the shoe for a Newtonian fluid (Section 3), a power law fluid (Section 4), and a Bingham plastic (Section 5). This work demonstrates how the rheology of the mash is crucial for accurately predicting the shear stresses experienced during the flow under the shoe. Finally, in Section 6, we discuss the results and present some recommendations.

2 Modelling the flow under the shoe

For simplicity, we begin modelling the problem of flow under the shoe by expressing all positions and velocities in a frame that moves with the mould. That is, we write the problem mathematically as if the mould remains fixed and the shoe moves over the top of it, as illustrated in Figure 2. From Figure 2, we see that a flow of mash in the mould will be induced by the movement of the "lid" provided by the shoe. Hence, the flow of mash under the shoe can be thought of as an example of lid-driven cavity flow. This is a classic problem in fluid mechanics and detailed reviews can be found in [1, 2].
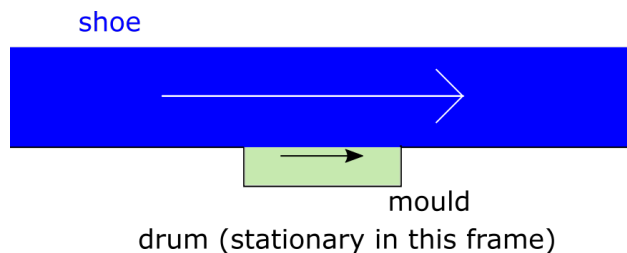

Figure 2: Schematic of a disk being transported under the shoe, treated in a frame where the mould is taken to be fixed while the shoe is treated as if it were moving. The shoe becomes like a lid moving across the top of a cavity, giving rise to lid-driven cavity flow.

While there is an extensive literature on lid-driven cavity flow, this mostly deals with Newtonian flows in geometries that are not directly relevant to our problem. Most commonly, papers on lid-driven cavity flow concern the calculation of certain flows for benchmarking the performance of numerical simulations. In the case of concern here, the problem of lid-driven cavity flow is fully three dimensional, making solutions challenging to compute, even if numerical methods are used. As described in [2], progress can be made with three-dimensional problems for Stokes flow (i.e., where viscous effects dominate over inertia); however, even in this case the solution is difficult to compute and interpret.

In describing the flow of mash under the shoe, we have one added challenge and one additional simplification that can be made. The added challenge is that the mash is unlikely

to behave as a Newtonian fluid. Experimental results indicate that the viscosity of the mash may change as a function of the shear rate and it is also possible that the mash may behave like a viscoelastic fluid. Additionally, the mash may exhibit some plastic behaviour; that is, the mash may behave like a solid until a sufficiently large shear is applied for the mash to flow. The fact that the mash is not a Newtonian fluid will be important to its flow properties and this presents mathematical challenges.

Despite these challenges, we are also able to make a useful simplification to our analysis of the flow. The additional simplification that we can make is due to a combination of the fact that the reduced Reynolds number of the flow will be very small (indicating that viscous effects will dominate inertial effects in the moulds) and the fact that the depth of an individual mould is significantly smaller than the lateral extent of an individual mould. Away from a turnover region (with width comparable to the depth of the moulds) near the sides of the moulds, it follows that the flow of mash will be well described by a one-dimensional lubrication approximation.

As we will see in Sections 4 and 5, the lubrication approximation is particularly powerful because it enables us to solve for the flow in the case of a non-Newtonian fluid such as a power-law fluid or a Bingham plastic. While the solutions we obtain will not apply near the sides of the mould, they will be useful for estimating the maximum shear stress and flow profile through most of the mash disk. In the rest of this section, we will sketch out the mathematical formulation of the lubrication approximation.

As outlined previously, we work in a frame where the position of the mould is fixed (and hence the shoe can be treated as moving). Let (x, y, z) be a spatial coordinate system as follows

- The x-axis is taken to be parallel to the direction of movement of the shoe, with x increasing in the direction of shoe movement.

- The y-axis is taken to be perpendicular to the shoe, with y increasing from the bottom of the mould to the shoe.

- The z-axis is taken to be perpendicular to the x and y axes, constructed to create a right-handed coordinate system.

We centre our axes so that the bottom surface of the mould is at $y = 0$ and the upper surface of the mould (the shoe) is at $y = h$. While it is essential that the mould has sides that prevent the leakage of mash, the location of these sides is irrelevant for the one-dimensional analysis that follows. We define u, v, and w to be the components of fluid velocity in the x, y, and z directions respectively.

There will be a turnover region near the sides of the mould where the flow is fully three-dimensional. Away from this turnover region, the flow will be governed by a lubrication approximation where the only nonzero component of velocity is u, the velocity in the x-direction. Taking p to be the pressure and $\tau(u_y)$ to be the x-y shear stress, this lubrication

approximation will take the form

$$\frac{\partial p}{\partial y} = 0, \qquad\qquad \frac{\partial u}{\partial x} = 0, \qquad\qquad \frac{\partial p}{\partial x} = \frac{\partial}{\partial y}\left[\tau\left(\frac{\partial u}{\partial y}\right)\right]. \qquad (1)$$

These equations must be solved subject to no-slip boundary conditions at $y = 0$ and $y = h$. Taking the velocity of the moving lid to be U, these boundary conditions take the form

$$u(x,0) = 0, \qquad\qquad u(x,h) = U. \qquad (2)$$

In addition to these boundary conditions, we require a condition on the total flux through any cross-section. Since the mould is a confined cavity with mash unable to enter or leave while it passes under the shoe, we require the flux through a surface that extends the full height of the mould to be zero, which gives

$$\int_0^h u(x,y)\,\mathrm{d}y = 0. \qquad (3)$$

From the equations in (1), we find that u will be a function of y only, and that $\frac{\mathrm{d}p}{\mathrm{d}x}$ will be constant. Letting $G = \frac{\mathrm{d}p}{\mathrm{d}x}$ represent the pressure gradient, we are left with the following one-dimensional system for the unknown function $u(y)$ and the unknown constant G:

$$G = \frac{\mathrm{d}}{\mathrm{d}y}\left(\tau\left(\frac{\mathrm{d}u}{\mathrm{d}y}\right)\right), \qquad (4\mathrm{a})$$

$$\int_0^h u(y)\,\mathrm{d}y = 0, \qquad (4\mathrm{b})$$

$$u(0) = 0, \qquad (4\mathrm{c})$$
$$u(h) = U. \qquad (4\mathrm{d})$$

The final element required to close this system is a constitutive law for the relationship between the shear-stress, τ, and the velocity gradient, $\frac{\mathrm{d}u}{\mathrm{d}y}$. For a Newtonian fluid, this constitutive law takes the simple form

$$\tau(u_y) = \mu\frac{\mathrm{d}u}{\mathrm{d}y}, \qquad (5)$$

where μ is a constant representing the viscosity. This enables (4a) to be simplified to

$$G = \mu\frac{\mathrm{d}^2 u}{\mathrm{d}y^2}. \qquad (6)$$

As outlined in Section 3, this makes solution of (4) relatively straight forward.

In addition to this, we can consider more complicated rheologies. In Section 4, we consider the possibility that the mash is best described as a power-law fluid. In this case, the constitutive law would be

$$\tau(u_y) = \mu \left(\frac{\mathrm{d}u}{\mathrm{d}y} \right) \frac{\mathrm{d}u}{\mathrm{d}y}, \tag{7}$$

where $\mu[u_y]$ is the viscosity, which is dependent on the shear rate, u_y. For a power-law fluid, this takes the form $\mu[u_y] = K|u_y|^n$, where K and n are constants.

The last possibility that we consider is that the mash can be treated as a Bingham plastic. For a Bingham plastic, the relationship between stress and shear rate depends on whether a critical threshold has been exceeded. For stresses with magnitude below the yield stress, τ^*, the material behaves rigidly and the shear rate is zero. Beyond this yield stress, the material flows so that the shear rate is proportional to the difference between the stress and the yield stress. We formulate this mathematically and discuss it further in Section 5.

3 Solution of the flow under the shoe for a Newtonian fluid

For a Newtonian fluid, the equations of motion for the fluid (including boundary conditions) from (4) become

$$G = \mu \frac{\mathrm{d}^2 u}{\mathrm{d}y^2}, \tag{8a}$$

$$\int_0^h u(y)\,\mathrm{d}y = 0, \tag{8b}$$

$$u(0) = 0, \tag{8c}$$

$$u(h) = U. \tag{8d}$$

Integrating (8a) twice and applying the boundary conditions (8c) and (8d), we obtain a solution of

$$u(y) = \frac{G}{2\mu}y^2 + \left(\frac{U}{h} - \frac{Gh}{2\mu} \right) y. \tag{9}$$

We recall that the constant G needs to be determined. This can be found by integrating (9) and applying (8b). This gives

$$0 = \int_0^h u(y)\,\mathrm{d}y = \frac{Uh}{2} - \frac{Gh^3}{12\mu}.$$

In order to satisfy this, we find that

$$G = \frac{6\mu U}{h^2}. \tag{10}$$

Substituting into (9), this gives the solution for the velocity as

$$u(y) = U\left(\frac{3y^2}{h^2} - \frac{2y}{h}\right). \tag{11}$$

The associated shear stress, $\tau = \mu\frac{\mathrm{d}u}{\mathrm{d}y}$, is

$$\tau(y) = \frac{U\mu}{h}\left(\frac{6y}{h} - 2\right). \tag{12}$$

Hence we find that the maximum shear stress occurs at the upper surface $y = h$, where the mash is in contact with the shoe. This is a common feature of all of the flows that we investigate; the maximum shear stress always occurs at the boundary with the shoe. In the case of a Newtonian fluid, this maximum shear stress can be expressed explicitly:

$$\tau_{\max} = \frac{4U\mu}{h}. \tag{13}$$

Since the Newtonian fluid can be thought of as a special case of a power-law fluid (where $n = 1$) and a special case of a Bingham plastic (where $\tau^* = 0$), plots of the velocity profile for a Newtonian fluid are given in both Figure 3 and Figure 4 for comparison with other solutions.

4   Solution of the flow under the shoe for a power-law fluid

Consider now that the fluid can be modelled as a power-law fluid, that is we can write the effective viscosity in the form

$$\mu = K\left|\frac{\partial u}{\partial y}\right|^{n-1}, \tag{14}$$

for constants K and n. The values of K and n can be determined from rheology testing. Data were supplied during the study group based on rheological measurements at different shear rates. Some of these results indicate that a power-law fluid is a good fit to measured behaviour, although we note that more experimentation is required to conclude whether the non-Newtonian behaviour observed is most consistent with this or with some other rheology.

As for the Newtonian case above, we exploit the small aspect ratio in the mould and

adopt a lubrication approximation which gives our governing equations as

$$G = \frac{\mathrm{d}}{\mathrm{d}y}\left(\mu\left(\frac{\mathrm{d}u}{\mathrm{d}y}\right)\frac{\mathrm{d}u}{\mathrm{d}y}\right) \qquad \text{for } 0 \leq y \leq a, \tag{15}$$

$$u(0) = 0, \tag{16}$$

$$u(h) = U, \tag{17}$$

$$\int_0^h u(y)\,\mathrm{d}y = 0, \tag{18}$$

where the boundary conditions correspond to no-slip on the base and the shoe, and conservation of mass. Care must be taken with (15) in order to ensure the correct sign is used on the right hand side from (14). It proved most straight-forward to divide the flow into two regions in which $\partial u/\partial y$ was either positive or negative. Defining the velocities in each region as u_1 and u_2, and defining a to be the y value at which $\frac{\mathrm{d}u}{\mathrm{d}y} = 0$, we can integrate (15) once directly to obtain the following problem to solve:

$$K^{\frac{1}{n}}\frac{du_1}{dy} = -(c_1 - Gy)^{\frac{1}{n}}, \qquad \text{for } 0 \leq y \leq a \tag{19}$$

$$K^{\frac{1}{n}}\frac{du_2}{dy} = (Gy - c_3)^{\frac{1}{n}}, \qquad \text{for } a \leq y \leq h \tag{20}$$

$$u_1(0) = 0, \tag{21}$$

$$u_2(h) = U, \tag{22}$$

$$\frac{du_1}{dy} = 0, \qquad \text{at } y = a, \tag{23}$$

$$\frac{du_2}{dy} = 0, \qquad \text{at } y = a, \tag{24}$$

$$u_1(a) = u_2(a), \tag{25}$$

$$\int_0^h u(y)\,\mathrm{d}y = 0, \tag{26}$$

with unknown constants of integration c_1 and c_3, and where the additional boundary conditions come from matching the velocities in the two regions at the unknown transition point $y = a$.

We can integrate the differential equations for the velocity immediately to obtain

$$K^{\frac{1}{n}}u_1 = \frac{n}{1+n}\frac{1}{G}(c_1 - Gy)^{\frac{1+n}{n}} + c_2, \tag{27}$$

$$K^{\frac{1}{n}}u_2 = \frac{n}{1+n}\frac{1}{G}(Gy - c_3)^{\frac{1+n}{n}} + c_4, \tag{28}$$

To simplify the algebra, we rewrite the pressure gradient by introducing $\tilde{P} = \frac{hG}{c_1}$, leaving

$$K^{\frac{1}{n}} u_1 = \frac{n}{1+n} \frac{hc_1^{\frac{1}{n}}}{\tilde{P}} \left(1 - \tilde{P}\frac{y}{h}\right)^{\frac{1+n}{n}} + c_2, \tag{29}$$

$$K^{\frac{1}{n}} u_2 = \frac{n}{1+n} \frac{hc_1^{\frac{1}{n}}}{\tilde{P}} \left(\tilde{P}\frac{y}{h} - \frac{c_3}{c_1}\right)^{\frac{1+n}{n}} + c_4. \tag{30}$$

In order to satisfy (23) we require $\tilde{P} = h/a$ and to satisfy (24) we need $c_3 = c_1$. Additionally (21) fixes

$$c_2 = -\frac{n}{1+n} \frac{hc_1^{\frac{1}{n}}}{\tilde{P}}, \tag{31}$$

and (22) fixes

$$c_4 = K^{\frac{1}{n}} U - \frac{n}{1+n} \frac{hc_1^{\frac{1}{n}}}{\tilde{P}} \left(\tilde{P} - 1\right)^{\frac{1+n}{n}}. \tag{32}$$

We can then determine c_1 by imposing (25) to give

$$c_1^{\frac{1}{n}} = \frac{n+1}{n} \frac{K^{\frac{1}{n}} U}{a \left(\frac{h}{a} - 1\right)^{\frac{1+n}{n}} - a}$$

yielding our velocities in terms of one remaining unknown a

$$u_1 = \frac{U}{\left(\frac{h}{a} - 1\right)^{\frac{1+n}{n}} - 1} \left(\left(1 - \frac{y}{a}\right)^{\frac{1+n}{n}} - 1\right), \tag{33}$$

$$u_2 = \frac{U}{\left(\frac{h}{a} - 1\right)^{\frac{1+n}{n}} - 1} \left(\left(\frac{y}{a} - 1\right)^{\frac{1+n}{n}} - \left(\frac{h}{a} - 1\right)^{\frac{1+n}{n}}\right) + U, \tag{34}$$

We still need to satisfy the flux requirement (26):

$$\int_0^h u(y)\,dy = \int_0^a u_1(y)\,dy + \int_a^h u_2(y)\,dy = 0. \tag{35}$$

This can be used to find a (or, more naturally, the dimensionless parameter $\frac{h}{a}$). In general, we note that $\frac{h}{a}$ depends only on n and is independent of the other model parameters.

Expanding (35) and simplifying, we find that $\frac{h}{a}$ must satisfy

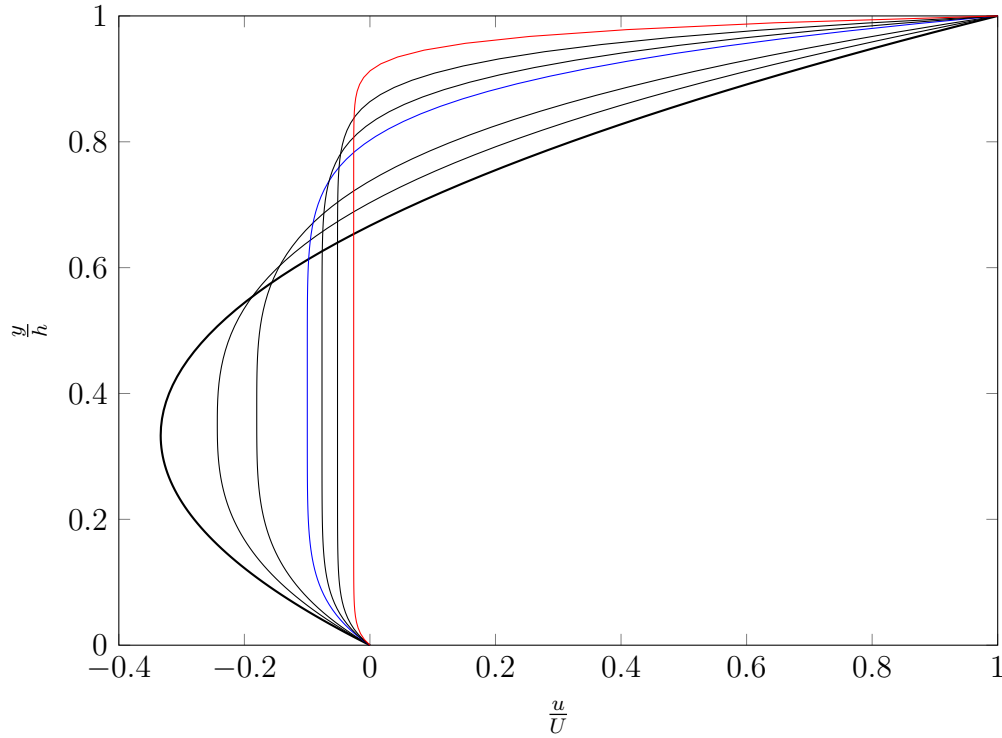$$\left(\frac{h}{a} - 1\right)^{\frac{2n+1}{n}} - \frac{2n+1}{n} \cdot \frac{h}{a} + 1 = 0. \tag{36}$$

Figure 3: Velocity profile u/U against vertical position y/h for power law fluids with $n = 1$ (the Newtonian case, shown as a thick line), $n = 0.6$, $n = 0.4$, $n = 0.2$ (shown in blue), $n = 0.15$, $n = 0.1$, and $n = 0.05$ (shown in red).

In the case where $\frac{1}{n}$ is an integer, this can be expanded to obtain a polynomial of degree $\frac{1}{n} + 2$ with a double root at zero. Factorising this double root out, we find that $\frac{h}{a}$ will satisfy the polynomial

$$\sum_{k=0}^{n} (-1)^k \binom{n+2}{k} \left(\frac{h}{a}\right)^{n-k} = 0. \tag{37}$$

The velocity profiles for different values of n are shown in Figure 3. Note that as n becomes closer to zero, we approach a system where there is a large part of the mash that is effectively moving at the same speed (seen from the flatness of the middle of the velocity profile). This is comparable to the results that we find in Section 5 for a Bingham plastic.

The pressure gradient is given by

$$G = \frac{\tilde{P}c_1}{h} = \frac{c_1}{a} = \frac{KU^n}{h^{n+1}} \cdot \frac{(n+1)^n \left(\frac{h}{a}\right)^{n+1}}{\left(\left[\frac{h}{a} - 1\right]^{\frac{1+n}{n}} - 1\right)^n n^n}. \tag{38}$$

As previously, the maximum shear occurs at $y = h$. We find that the maximum shear

stress is given by

$$\tau_{\max} = K \left(\left. \frac{\mathrm{d}u}{\mathrm{d}y} \right|_{y=h} \right)^n = \frac{KU^n}{h^n} \cdot \frac{\left(\frac{h}{a} \right)^n \left(\frac{h}{a} - 1 \right) (n+1)^n}{\left(\left[\frac{h}{a} - 1 \right]^{\frac{n+1}{n}} - 1 \right)^n n^n} \tag{39}$$

Since $\frac{h}{a}$ depends only on n, the complicated term in the second fraction is a prefactor that depends only on n; it can be evaluated based solely on the type of power law fluid being studied. Note also that, unlike the Newtonian case, the maximum shear stress is proportional to U^n rather than to U and inversely proportional to h^n rather than to h. This is consistent with what we would expect from dimensional analysis, and the implications of this result will be discussed in Section 6.

5 Solution of the flow under the shoe for a Bingham plastic

Lastly, we consider the case where the fluid is a Bingham plastic. A Bingham plastic behaves rigidly (i.e., there is zero shear rate) when the magnitude of the shear stress is below some critical threshold, τ^*. As the shear stress increases beyond this threshold, the shear rate increases linearly in proportion to the difference between the magnitude of the shear stress and τ^*. Expressed mathematically for our problem (where the shear rate is $\frac{\mathrm{d}u}{\mathrm{d}y}$), we obtain

$$\frac{\mathrm{d}u}{\mathrm{d}y} = \begin{cases} \frac{\tau + \tau^*}{\mu}, & \tau < -\tau^*, \\ 0, & |\tau| \leq \tau^*, \\ \frac{\tau - \tau^*}{\mu}, & \tau > \tau^*, \end{cases} \tag{40}$$

where μ is the viscosity.

Under the hypothesis of unidirectional (lubrication) flow, we have from equation (4a) that

$$G = \frac{\mathrm{d}\tau}{\mathrm{d}y}, \tag{41}$$

where G is the unknown constant pressure gradient, $\frac{\mathrm{d}p}{\mathrm{d}x}$. Integrating in y, we obtain a linear relationship between the shear stress and vertical position:

$$\tau = G(y - \bar{y}), \tag{42}$$

where $\bar{y}$ is the height at which $\tau = 0$.

We define two heights y_1 and y_2 such that the fluid yields below y_1 and above y_2. That is, these are the heights at which $|\tau| = \tau^*$. This means that

$$\tau^* = G(\bar{y} - y_1), \qquad\qquad \tau^* = G(y_2 - \bar{y}), \tag{43}$$

and these can be combined to give

$$2\tau^* = G(y_2 - y_1). \tag{44}$$

As in Section 4, it is convenient to break the domain $(0, h)$ into different subdomains and solve for u separately in these domains. We define functions $u_1(y)$ and $u_2(y)$ and constant u^* so that

$$u = \begin{cases} u_1(y), & 0 \le y \le y_1, \\ u^*, & y_1 \le y \le y_2, \\ u_2(y), & y_2 \le y \le h. \end{cases} \tag{45}$$

Note that u^* can be physically interpreted as the velocity of the rigid plug within the Bingham plastic flow. We expect $u^* < 0$ since this will be part of the returning flow.

Starting from equation (40) and applying (42) and (43), we find that when $0 \le y \le y_1$ we have

$$\frac{du_1}{dy} = \frac{G}{\mu}(y - y_1). \tag{46}$$

Integrating, and noting that $u_1(y_1) = u^*$ for continuity of u this gives

$$u_1(y) = u^* + \frac{G}{2\mu}(y - y_1)^2. \tag{47}$$

Since $u_1(0) = 0$ from (4c), we find that

$$u^* = -\frac{G}{2\mu}{y_1}^2. \tag{48}$$

Similarly, when $y_2 \le y \le h$ we find that

$$\frac{du_2}{dy} = \frac{G}{\mu}(y - y_2), \tag{49}$$

which integrates to give

$$u_2(y) = u^* + \frac{G}{2\mu}(y - y_2)^2. \tag{50}$$

Since $u_2(h) = U$ from (4d), we find that

$$U = u^* + \frac{G}{2\mu}(h - y_2)^2. \tag{51}$$

Note that (48) and (51) can be combined to give

$$U = \frac{G}{2\mu}\left([h - y_2]^2 - {y_1}^2\right) \tag{52}$$

From (47) and (50), we find that the overall velocity profile is

$$u(y) = \begin{cases} u^* + \frac{G}{2\mu}(y - y_1)^2, & 0 \le y \le y_1 \\ u^*, & y_1 \le y \le y_2, \\ u^* + \frac{G}{2\mu}(y - y_2)^2, & y_2 \le y \le h. \end{cases} \tag{53}$$

However, this is not (at this stage) a particularly useful solution, since it contains many parameters still to be determined. At this stage, we have not specified a method for finding u^*, G, y_1 or y_2.

This can be resolved by using (4b). Integrating, we find

$$0 = \int_0^{y_1} u_1(y)\,\mathrm{d}y + (y_2 - y_1)u^* + \int_{y_2}^h u_2(y)\,\mathrm{d}y, \tag{54}$$

$$= u^* h + \frac{G}{6\mu} y_1{}^3 + \frac{G}{6\mu}(h - y_2)^3. \tag{55}$$

Using (48) to substitute for u^*, this becomes

$$0 = \frac{G}{6\mu}\left(-3y_1{}^2 h + y_1{}^3 + [h - y_2]^3\right), \tag{56}$$

which implies

$$y_2 = h - \sqrt[3]{3y_1{}^2 h - y_1{}^3}. \tag{57}$$

This can be substituted into (52) to obtain

$$U\mu = \frac{G}{2}\left([3y_1{}^2 h - y_1{}^3]^{\frac{2}{3}} - y_1{}^2\right), \tag{58}$$

and into (44) to obtain

$$\tau^* = \frac{G}{2}\left(h - \sqrt[3]{3y_1{}^2 h - y_1{}^3} - y_1\right). \tag{59}$$

Taking the quotient of (58) and (59) and rearranging yields

$$\frac{\tau^* h}{U\mu} = \frac{1 - \sqrt[3]{3(y_1/h)^2 - (y_1/h)^3} - y_1/h}{[3(y_1/h)^2 - (y_1/h)^3]^{\frac{2}{3}} - (y_1/h)^2}. \tag{60}$$

While nonlinear and unpleasant, this is a single algebraic equation that must be solved for the dimensionless constant $\frac{y_1}{h}$ when the known dimensionless critical shear stress $\frac{\tau^* h}{U\mu}$ is specified.
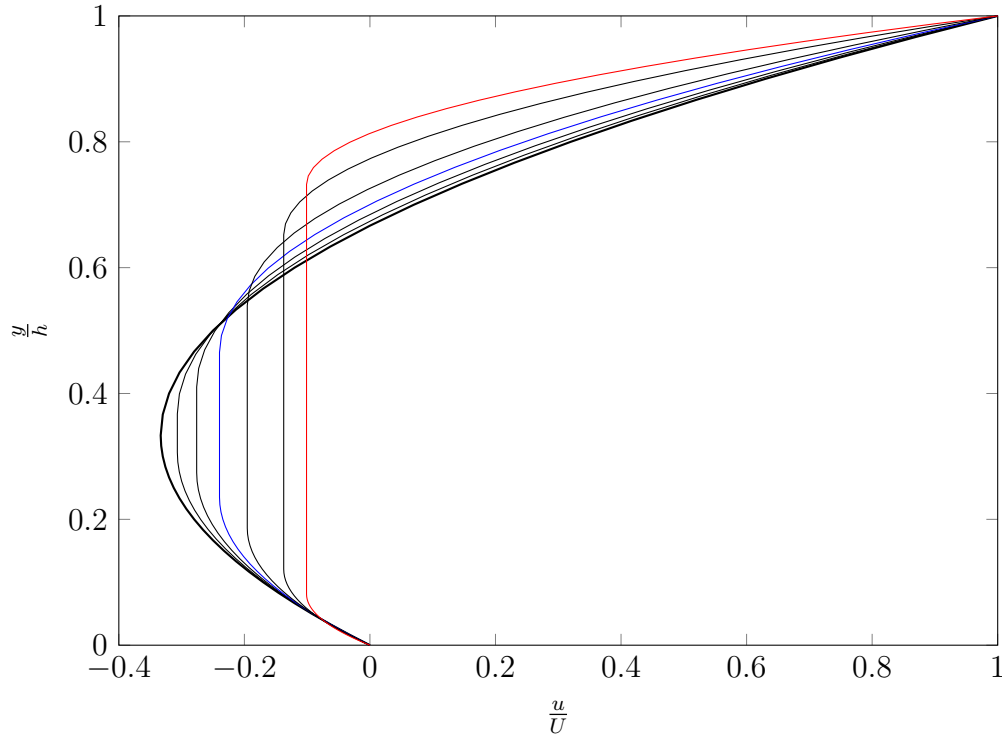
Figure 4: Plots of velocity profile in the mash for a Bingham plastic for different values of the dimensionless critical shear stress, $\frac{\tau^* h}{U\mu}$. Figures shown are $\frac{\tau^* h}{U\mu} = 0$ (the Newtonian case, shown with a thick line), $\frac{\tau^* h}{U\mu} = 0.2$, $\frac{\tau^* h}{U\mu} = 0.5$, $\frac{\tau^* h}{U\mu} = 1$ (shown in blue), $\frac{\tau^* h}{U\mu} = 2$, $\frac{\tau^* h}{U\mu} = 5$, and $\frac{\tau^* h}{U\mu} = 10$ (shown in red). Note that as $\frac{\tau^* h}{U\mu}$ increases, the size of the region where $u = u^*$ also increases.

Once $\frac{y_1}{h}$ is obtained by solving (60), the other constants G, u^* and y_2 can be obtained directly from $\frac{y_1}{h}$ using the following:

$$G = \frac{U\mu}{h^2} \cdot \frac{2}{[3(y_1/h)^2 - (y_1/h)^3]^{\frac{2}{3}} - (y_1/h)^2}, \tag{61}$$

$$u^* = -U \cdot \frac{(y_1/h)^2}{[3(y_1/h)^2 - (y_1/h)^3]^{\frac{2}{3}} - (y_1/h)^2}, \tag{62}$$

$$y_2 = h \cdot \left(1 - [3(y_1/h)^2 - (y_1/h)^3]^{\frac{1}{3}}\right). \tag{63}$$

These can then be substituted back into (53) to obtain the full solution. Solutions for a range of values of $\frac{\tau^* h}{U\mu}$ are shown in Figure 4

As previously, the maximum shear stress occurs at $y = h$. For the Bingham plastic, we

find that

$$\tau_{\max} = \tau^* + G(h - y_2) \tag{64}$$

$$= \tau^* + \frac{U\mu}{h} \cdot \frac{2\left[3(y_1/h)^2 - (y_1/h)^3\right]^{\frac{1}{3}}}{\left[3(y_1/h)^2 - (y_1/h)^3\right]^{\frac{2}{3}} - (y_1/h)^2} \tag{65}$$

$$= \frac{U\mu}{h} \cdot \left(\frac{\tau^* h}{U\mu} + \frac{2\left[3(y_1/h)^2 - (y_1/h)^3\right]^{\frac{1}{3}}}{\left[3(y_1/h)^2 - (y_1/h)^3\right]^{\frac{2}{3}} - (y_1/h)^2}\right) \tag{66}$$

Unfortunately, this expression is not immediately informative because of the complicated problem to be solved for $\frac{y_1}{h}$. If we are concerned with what will happen to the maximum shear stress as the speed of the process (and hence U) increases while the shear stress (and hence τ^*) remains fixed, it is useful to think about the proportional increase from the critical shear stress to the maximum shear stress. Using (65), we observe that

$$\frac{\tau_{\max} - \tau^*}{\tau^*} = \frac{U\mu}{\tau^* h} \cdot \frac{2\left[3(y_1/h)^2 - (y_1/h)^3\right]^{\frac{1}{3}}}{\left[3(y_1/h)^2 - (y_1/h)^3\right]^{\frac{2}{3}} - (y_1/h)^2}. \tag{67}$$

Since $\frac{y_1}{h}$ can be expressed as a function of $\frac{U\mu}{\tau^* h}$ only using (60), this gives us a way of expressing information about the dependence of $\tau_{\max}$ on U in a single plot. This is shown in Figure 5

We note that this looks suspiciously close to being a straight line. We have not yet found a good reason for the relationship between maximum shear stress and velocity to be linear in this manner, although we suspect that this may be associated with the asymptotic behaviour of the solution for large values of $\frac{U\mu}{\tau^* h}$. A suitable line of best fit (shown in Figure 5 in blue) appears to be

$$\frac{\tau_{\max} - \tau^*}{\tau^*} = 4 \cdot \frac{U\mu}{\tau^* h} + 0.6, \tag{68}$$

and hence the maximum shear stress can be estimated as

$$\tau_{\max} = 4\frac{U\mu}{h} + 1.6\tau^*. \tag{69}$$

This compares well with the Newtonian results, $\tau_{\max} = 4\frac{U\mu}{h}$; essentially, the role of the critical shear stress, τ^*, is to increase the maximum shear stress by an amount proportional to τ^*.

Asymptotic solutions may be obtained for the velocity profiles and maximum shear stresses in the case where $\frac{\tau^* h}{U\mu}$ is very large, and the flow is essentially a plug flow with small shear layers on either side) and for the case where $\frac{\tau^* h}{U\mu}$ is very small (and the flow is close to being Newtonian), but this work was not finalised during the study group and is not discussed in this report. Asymptotic analysis of this problem may be useful for explaining the linear trend observed in Figure 5.
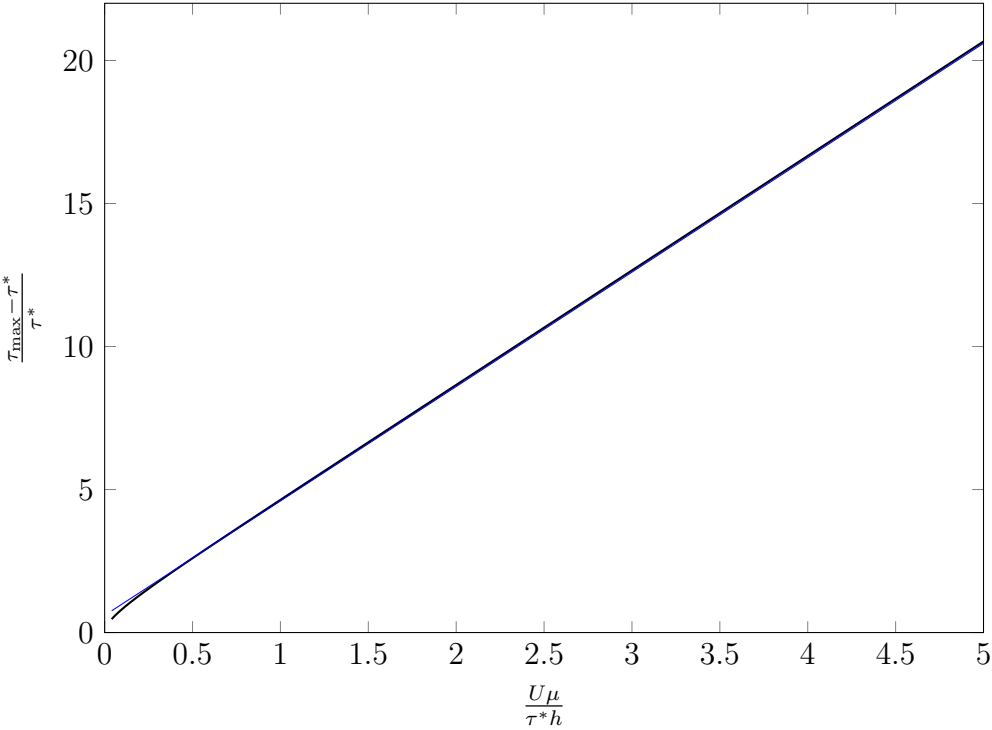
Figure 5: Plot of a dimensionless form of the maximum stress, $\frac{\tau_{\max} - \tau^*}{\tau^*}$ as a function of dimensionless shoe velocity, $\frac{U\mu}{\tau^* h}$ shown as a thick black line. The line of best fit (valid for large values of $\frac{U\mu}{\tau^* h}$) from equation (68) is shown in blue.

6   Discussion and conclusions

This report presents an analysis of an industrial process by which mash is moulded into disks. The main focus of our analysis was the maximum shear stress experienced by the mash in the disks as they pass under a fixed upper surface (the shoe). Since the mash is a complex material and the moulds are shallow relative to their width, we focused on developing one-dimensional solutions to the flow problem that can be adapted to different constitutive laws for the mash rather than looking at the fully three-dimensional lid-driven cavity flow that takes place in individual moulds.

We considered three different constitutive laws for the mash: a Newtonian fluid model, a power-law fluid model (suitable for a mash whose viscosity changes as the shear rate increases), and a Bingham plastic model (suitable for a mash that behaves as a solid until a certain shear stress is applied). We found that, in all cases, the maximum shear stress occurs at the surface in contact with the shoe. Depending on the constitutive law of the mash, we were able to obtain formulae for this maximum stress; see, for example, (13) for a Newtonian fluid and (39) for a power-law fluid.

Importantly, the maximum shear stress depends on the velocity at which the mould moves past the shoe, U. In the case of a Newtonian fluid, $\tau_{\max} = \frac{4U\mu}{h}$, while for a power-law fluid $\tau_{\max} \propto U^n$. If $n < 1$ (as it will be for a shear-thinning fluid), this indicates that the dependence of maximum shear stress on U is not as dramatic as it would be for a Newtonian fluid.

In the case of a Bingham plastic, we obtained an approximate solution that suggests that $\tau_{\max} \approx 4\frac{U\mu}{h} + 1.6\tau^*$, where U is the velocity at which the mould moves past the shoe, μ is the viscosity, h is the depth of the mould, and τ^* is the critical shear stress for the Bingham model. This is a surprisingly simple result that warrants further investigation. Detailed work in this area (including asymptotic analysis of the cases where the critical stress τ^* is small or large) would be a good mathematical extension of the work achieved so far but was not achieved during the study group.

From a mathematical perspective, there is a significant amount of other further work that could be done. Some of the rheological data available at the study group suggested that the mash might behave as a viscoelastic fluid. While we considered a range of constitutive laws for the mash, our analysis did not include any viscoelastic constitutive laws; while more complicated, such analysis may be worthwhile if rheological studies suggest that a viscoelastic model is more appropriate than a power-law or Bingham model.

Even without considering other constitutive laws, there is further mathematical analysis that could be done with the current results. It may be interesting to consider the "turnover rate"; that is, the flux of fluid in the region where $u > 0$ (or equally where $u < 0$). This could be used to estimate the number of times a given fluid particle will circulate as the mash passes under the shoe. While our focus was on the maximum shear, the turnover rate may be important for the effective mixing of the mash as it passes under the shoe.

In conclusion, a one-dimensional model of flow in a mould is useful for providing insights such as the maximum shear stress and the flow profile. Importantly, a one-dimensional model is simple enough to facilitate exploring the effects of different constitutive laws; in the problem described here, the fact that the mash is not a conventional Newtonian fluid is likely to have a more significant impact on the flow than variations in the flow profile around the disk. We recommend further rheological study of the mash, and possibly further modelling work (especially if it becomes apparent that a viscoelastic model of the fluid is more appropriate than either a power-law or a Bingham model). Overall, this is a good example of a problem where mathematical modelling can be used to analyse the key features of the flow.

References

[1] Hendrik C. Kuhlmann and Francesco Romanò. The lid-driven cavity. In *Computational Methods in Applied Sciences*, pages 233–309. Springer International Publishing, 2018.

[2] P. N. Shankar and M. D. Deshpande. Fluid mechanics in the driven cavity. *Annual Review of Fluid Mechanics*, 32(1):93–136, 2000.

Acknowledgements